THE JOURNAL OF BIOLOGICAL CHEMISTRY
Vol. 276, No. 31, Issue of August 3, pp. 28999–29006, 2001
Printed in U.S.A.

Defining a Link between Gap Junction Communication, Proteolysis, and Cataract Formation*

Received for publication, April 24, 2001, and in revised form, May 30, 2001
Published, JBC Papers in Press, June 6, 2001, DOI 10.1074/jbc.M103628200

Amos Baruch‡§, Doron Greenbaum‡, Esther T. Levy§, Peter A. Nielsen§, Norton B. Gilula§, Nalin M. Kumar§¶, and Matthew Bogyo‡‖

From the ‡Department of Biochemistry and Biophysics, University of California, San Francisco, California 94143 and the §Department of Cell Biology, Scripps Research Institute, La Jolla, California 92037

Disruption of the connexin α3 (Cx46) gene (α3 (−/−)) in mice results in severe cataracts within the nuclear portion of the lens. These cataracts are associated with proteolytic processing of the abundant lens protein γ-crystallin, leading to its aggregation and subsequent opacification of the lens. The general cysteine protease inhibitor, E-64, blocked cataract formation and γ-crystallin cleavage in α3 (−/−) lenses. Using a new class of activity-based cysteine protease affinity probes, we identified the calcium-dependent proteases, m-calpain and Lp82, as the primary targets of E-64 in the lens. Profiling changes in protease activities throughout cataractogenesis indicated that Lp82 activity was dramatically increased in α3 (−/−) lenses and correlated both spatially and temporally with cataract formation. Increased Lp82 activity was due to calcium accumulation as a result of increased influx and decreased outflux of calcium ions in α3 (−/−) lenses. These data establish a role for α3 gap junctions in maintaining calcium homeostasis that in turn is required to control activity of the calcium-dependent cysteine protease Lp82, shown here to be a key initiator of the process of cataractogenesis.

Gap junctions are formed by two hexameric structures of connexin molecules (connexons) that interact with connexons in neighboring cells to form membrane aqueous pores (1). These channels allow transfer of small molecules between the cytoplasm of neighboring cells. A number of studies have shown that communication facilitated by gap junctions is important both during embryonic development and for maintaining normal physiological functions within a cell (1, 2). However, the exact molecular mechanism by which gap junction communication contributes to these processes is still obscure.

In recent years, the vertebrate lens has been used extensively to study gap junction communication (3). The lens is a cellular, avascular organ made up predominantly of elongated fiber cells that are formed by the differentiation of epithelial cells that line the anterior surface of the developing lens. During differentiation, fiber cells lose their cytoplasmic organelles and begin to express lens-specific proteins know as crystallins. With age, this differentiation program gives rise to a spherical conglomerate of cells made up of concentric layers of fiber cells. As new layers form, older primary fiber cells are compressed inward, forming a central "nuclear region" of the mature lens.

In the vertebrate lens, each cell is coupled to its neighbors via gap junctions, resulting in a network of cell-cell contacts that has been suggested to be important for the maintenance of ion flux and for metabolic cooperation between the peripheral lens cells and the interior fiber cells (4). Three connexin genes are expressed in the vertebrate lens; epithelial cells express α1 (Cx43)[1] connexin; fiber cells express α3 (Cx46) and α8 (Cx50) connexin (5, 6).

In order to establish a functional role for gap junctions in the lens, connexin knockout mice have been generated (7, 8). Disruption of the α3 (Cx46) or α8 (Cx50) genes gives rise to distinct phenotypes; α8 ablation in mice results in reduced lens size (microphthalmia), and α3 knockout (α3 (−/−)) mice develop nuclear cataracts within 2 weeks of birth. Significantly, mutations in either α3 or α8 connexins are linked to congenital cataracts in humans (9, 10).

Structural integrity of the abundant lens proteins known as crystallins is necessary for maintaining the lens' refractive index. Perturbations in crystallin structure have been linked to cataract formation (11, 12). Specifically, γ-crystallin cleavage is associated with congenital, juvenile, and senile human cataracts (13, 14).

Initial characterization of the phenotype of α3 (−/−) mice indicated that lens opacity was associated with an accumulation of γ-crystallin cleavage products, leading to the formation of an insoluble conglomerate of disulfide-associated polypeptides (7). This increased cleavage of crystallin molecules in the lenses of α3 (−/−) mice suggested a critical role for proteolysis during the process of cataractogenesis.

Several forms of cataracts are directly associated with perturbations in the levels of calcium within the lens, indicating a potential role for the calcium dependent cysteine proteases known as calpains (15–17). Numerous reports have described the use of a general cysteine protease inhibitor, E-64, in experimental studies of cataract formation. E-64 inhibits cataract formation in cultured lenses treated with cataract-inducing agents such as diamide, selenite, and calcium ionophore (18, 19). However, the specific protein targets of this inhibitor in the lens were not identified, and tools for measuring activity of

* This work was supported by National Institutes of Health Grants GM37904 and Ey12142 (to A. B., N. B. G., and N. M. K.) and by funding from the Sandler Program in Basic Sciences (to M. B. and D. G.). The costs of publication of this article were defrayed in part by the payment of page charges. This article must therefore be hereby marked "*advertisement*" in accordance with 18 U.S.C. Section 1734 solely to indicate this fact.

¶ To whom correspondence may be addressed: Dept. of Cell Biology, Scripps Research Inst., La Jolla, CA 92037. Tel.: 858-784-2343; E-mail: nalin@scripps.edu.

‖ To whom correspondence may be addressed: Campus Box 0448, Dept. of Biochemistry and Biophysics, University of California, San Francisco, 513 Parnassus Ave., San Francisco, CA 94122. Tel.: 415-502-8142; E-mail: mbogyo@biochem.ucsf.edu.

[1] The abbreviations used are: Cx, connexin; AAH, artificial aqueous humor; NLVS, 5-iodo-4-hydroxy-3-nitrophenyl-acetyl-leucinyl-leucinyl-leucine vinyl sulfone; PAGE, polyacrylamide gel electrophoresis; WT, wild type; TBST, Tris-buffered saline with Tween 20; Z-VAD, Z-Val-Ala-Asp(OMe)-fluoromethyl ketone.

specific proteases *in situ* were lacking.

Recently, new biochemical reagents have been generated that allow the monitoring of global changes in protease activity. These reagents take advantage of the broad reactivity of the natural product E-64 to create chemical probes that covalently react with the papain family of cysteine proteases in an activity-dependent manner (20). Thus, labeling intensity can be used to determine relative activities of multiple proteases within a sample extract or tissue. In the present study, we have employed this labeling approach to identify the lens-specific calpain Lp82 and m-calpain as the predominant targets of E-64 in the mouse lens. Furthermore, *in situ* activity profiling of intact α3 (−/−) lenses revealed that, whereas m-calpain and Lp82 are expressed in both wild type and α3 (−/−) lenses, only Lp82 activity correlated with cataract formation. We therefore propose that calcium accumulation and the subsequent activation of the lens-specific calpain Lp82 in the α3 (−/−) lens are key events leading to cataract formation. These studies also provide a functional link between α3 gap junctions and maintenance of calcium homeostasis in the lens.

EXPERIMENTAL PROCEDURES

Reagents and Antibodies—E-64 was purchased from Calbiochem. Z-VAD was purchased from Enzyme System Products. DCG-03, DCG-04, ^{125}I-DCG-03, and ^{125}I-DCG-04 were synthesized as described (20). TC199 medium was purchased from Cellgro. The Vectastain kit (Vector Laboratories) was used to detect biotinylated proteases. Anti-Lp82 polyclonal antibodies were provided by T. R. Shearer (Oregon Health Sciences University, Portland, OR). Anti-m-calpain polyclonal antibodies were provided by J. S. Elce (Queen's University, Kingston, Ontario, Canada). Anti-μ-calpain monoclonal antibodies were provided by N. S. Kosower and S. Bar-Noy (Tel Aviv University, Tel Aviv, Israel).

Lens Homogenization and Western Blotting—Lenses were dissected from either WT or α(−/−) 129sv mice using a posterior approach. Wet weights were determined. Lenses were homogenized in 0.1 M NaCl, 50 mM Na_2HPO_4 (pH 7.0) at 40 mg of lens (wet weight/ml) of solution. An equal volume of 2× SDS sample buffer was added, and homogenates were incubated at 60 °C for 5 min. Samples (10 μl) were analyzed by 15% SDS-PAGE, blotted, and probed with anti-γ-crystallin antibodies.

Lens Organ Culture—Lenses from 1-week-old mice were dissected using the posterior approach in a microwell dissection dish containing 37 °C pre-warmed, serum-free TC199 medium supplemented with 250 units/ml penicillin and 25 μg/ml streptomycin. Lenses were incubated in a 24-well TC dish containing 1 ml/well TC199 at 37 °C in a humidified incubator under 5% CO_2. Protein concentration of the culture medium was determined 2 h after culturing to confirm that the lenses remained intact. Damaged lenses were discarded. For protease inhibition experiments, lenses were incubated as above in the presence of 100 μM E-64. Alternatively, lenses were incubated in the presence of 50 μM general caspase inhibitor Z-VAD.

^{125}I-DCG-04 Labeling in Vitro—Lenses were dissected as described above and homogenized in buffer A containing 50 mM Tris-HCl (pH 7.5), 1 mM EDTA, 1 mM EGTA, 2 mM dithiothreitol at 50 mg of lens (wet weight)/ml of solution. Labeling was performed using 100 μg of total protein/sample as described previously (20) in the presence or absence of various concentrations of free calcium (0–3 mM). The control proteasome label was used as described previously (21).

DCG-04 Labeling in Situ—Intact lenses from α3 (−/−) or WT mice were cultured as described above in the presence of 50 μM DCG-04 for 6 h. Incubation was performed in the presence or absence of 200 μM E-64 as indicated. Subsequently, lenses were homogenized in buffer A supplemented with 200 μM E-64. In some cases DCG-04-labeled lenses were subjected to immunoprecipitation using specific antibodies. Equal volume of 2× SDS sample buffer was added, and homogenates were boiled for 5 min. Homogenates were separated on a 9% acrylamide gel and transferred to a nitrocellulose membrane. Membranes were blocked in a 5% skim milk/TBST solution for 1 h at room temperature, followed by washing three times for 10 min each with TBST and incubation with Vectastain (Vector Laboratories) for 1 h. Subsequently, membranes were washed three times for 10 min each with TBST and analyzed using the Super Signal reagent (Pierce).

Measurement of Ion Concentrations—Lenses from WT, α3 (−/−), or α8 (−/−) mice were dissected and vacuum-dried for 48 h. In some cases the nuclear and cortical regions of the lens were dissected to give a wet weight ratio of 40:60, respectively, before drying. Pairs of dry lenses were then weighed and solubilized in 100 μl of 2% nitric acid for 12 h at 37 °C. De-ionized water was added to a final volume of 5 ml. The content of calcium, magnesium, and potassium was determined by inductively coupled plasma-optical emission spectrometry using a PerkinElmer Life Sciences 3000XL analyzer. All measurements were normalized to dry lens weight.

Measurement of Ca^{2+} Influx—Ca^{2+} influx measurements were performed as described previously (22). In brief, clear lenses from 10-day-old mice were pre-incubated at 35 °C for 2 h in artificial aqueous humor (AAH) containing: 130 mM NaCl, 5 mM KCl, 5 mM $NaHCO_3$, 1 mM $CaCl_2$, 0.5 mM $MgCl_2$, 5 mM glucose, and 20 mM HEPES (pH 7.25). Subsequently, medium was replaced with an AAH solution containing 2 μCi of ^{45}Ca and incubation continued for 2 h at 35 °C. Lenses were washed three times for 1 min each time in 5 ml of AAH, rolled on filter paper, and weighed. Lenses were homogenized in the presence of tissue solubilizer (Solusol; National Diagnostics) at 100 μl/lens pair and incubated for 1 h at 37 °C. Radioactivity of homogenates was measured in a liquid scintillation counter. Ca^{2+} influx was determined using the following equation.

$$Ca^{2+}\ \text{influx} = \frac{\text{cpm}_{\text{lens}}}{\text{cpm}_{\text{medium}}} \times \frac{[Ca^{2+}]_{\text{medium}}\, V_{\text{medium}}}{M_{\text{lens}}} \times \frac{1}{T} \qquad \text{(Eq. 1)}$$

cpm_{lens} = counts/min (cpm) measured in the lens, $\text{cpm}_{\text{medium}}$ = cpm measured in the medium, $[Ca^{2+}]_{\text{medium}}$ = concentration of calcium in the medium, V_{medium} = volume of the medium; M_{lens} = wet mass of the lens, and T = time of incubation with ^{45}Ca-containing solution.

Measurement of Ca^{2+} Outflux—Twelve pairs of clear lenses from 10-day-old WT or α3 (−/−) mice were incubated in the presence of AAH containing 2 μCi of ^{45}Ca. After 2 h of incubation, lenses were washed three times for 1 min each time in 5 ml of AAH and placed in 1 ml of fresh non-radioactive AAH. Lens cpm as well as medium cpm was determined after 2 h of incubation using a liquid scintillation counter. Initial lens cpm was calculated by adding lens cpm to medium cpm. Relative outflux units were calculated by subtracting the final lens cpm from the initial lens cpm and dividing by the initial lens cpm. Alternatively, the initial lens cpm was divided by the medium cpm. The two methods of calculation yielded the same results. The statistical average was obtained for the data collected from each pair. Two-tailed p values were determined using the Mann-Whitney unpaired test.

RESULTS

Characterization and Inhibition of γ-Crystallin Processing in α3 (−/−) Lenses—Connexin α3 (−/−) mice develop nuclear cataracts that further progress with age to dense nuclear opacities. To characterize the initial events leading to cataract formation, lenses from α3 (−/−) mice ranging in age from 1 to 4 weeks were analyzed (Fig. 1*A*). In all α3 (−/−) mice examined (>50), detectable lens opacity appeared between 10 and 14 days of age. Since γ-crystallin cleavage was previously reported to be associated with α3 (−/−) cataractogenesis (7), the processing of γ-crystallin was analyzed during the onset of cataracts (Fig. 1*B*). The initiation of cataracts coincided with the appearance of a previously reported low molecular weight γ-crystallin fragment (7). Further analyses of total lens homogenate using antibodies specific for crystallin αA, crystalline αB, and control cytoskeletal proteins did not reveal significant pattern differences between WT and α3 (−/−) lenses (data not shown).

To investigate the possibility that protease activation is a key event during α3 (−/−) cataractogenesis, we utilized a lens organ culture system. In this system, transparent lenses dissected from 1-week-old α3 (+/+) and α3 (−/−) mice were maintained for 1 week in culture. Although (+/+) lenses remained transparent during the entire 6-day incubation period, α3 (−/−) lenses developed a mild nuclear cataract after 2 days in culture, which progressed to a large, dense opacity.

In order to study the role of proteolysis in cataract formation, cultured lenses were incubated with several classes of protease inhibitors. The γ-crystallin cleavage site adjacent to an aspartic acid residue suggested that caspases might be involved in this process. However, neither cataractogenesis nor γ-crystallin

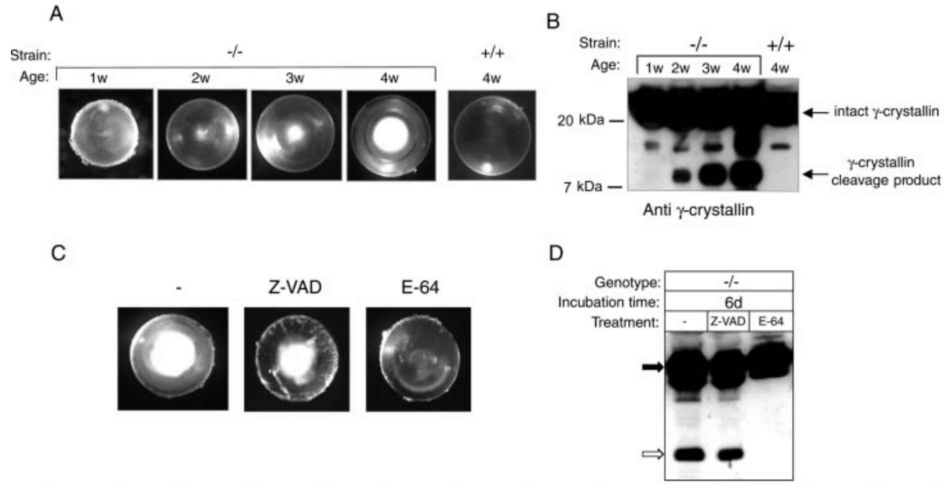

FIG. 1. **Cataract progression in the $\alpha 3$ (−/−) lens correlates with γ-crystallin cleavage and can be blocked by *ex vivo* treatment with the general papain family protease inhibitor E-64.** *A*, lenses dissected from 1-, 2-, 3-, and 4-week-old $\alpha 3$ (−/−) mice compared with a lens from a 4-week-old wild-type mouse. *B*, anti-γ-crystallin Western blot of extracts generated from lenses in *A*. *C*, treatment of 1-week-old WT and $\alpha 3$ (−/−) lenses with the general caspase inhibitor Z-VAD and the general papain family cysteine protease inhibitor, E-64. Lenses were treated with inhibitors for 6 h as described under "Experimental Procedures." *D*, anti-γ-crystallin Western blot of extracts generated from lenses in *C*. Size standards are indicated to the *left* of *panel B* (in kDa). The *upper* and *lower arrows* indicate the intact and cleaved γ-crystallin forms, respectively. *1w*, *2w*, *3w*, and *4w* represent age of mice in weeks.

cleavage was inhibited by the addition of the general caspase inhibitors, Z-VAD to $\alpha 3$ (−/−) cultured lenses (Fig. 1*C*). In agreement with these results, caspase activity, measured with several fluorogenic substrates, was located predominantly in the cortical region of the $\alpha 3$ (−/−) lenses, not the nuclear region associated with the cataracts (data not shown). Furthermore, eight different recombinant caspases (1, 2, 3, 5, 6, 7, 8, and 10) did not cleave γ-crystallin *in vitro* (data not shown). In contrast, incubation of $\alpha 3$ (−/−) lenses with low concentrations of the general cysteine protease inhibitor, E-64, completely blocked cataract formation (Fig. 1*C*) and inhibited γ-crystallin cleavage (Fig. 1*D*). No change in lens weight or hydration was observed in E-64-treated lenses (data not shown). These results indicate that cysteine protease(s) of the papain family are critical players in the process of cataractogenesis in the $\alpha 3$ (−/−) lens.

Profiling Cysteine Protease Activity in the Intact Lens—Having identified an inhibitor of cataract formation in $\alpha 3$ (−/−) lenses, our attention turned toward determining the molecular targets of this compound. Recently, our laboratory developed activity-based probes of the papain family of cysteine proteases based on the structure of the natural product, E-64 (20). The compounds (DCG-03 and DCG-04) are epoxide-containing, irreversible inhibitors that are tagged with both a biotin moiety and a site for attachment of a radioactive iodine residue (Fig. 2*A*). Proteins modified by these probes can be visualized by SDS-PAGE, followed by affinity blotting or by autoradiography.

Both DCG-03 and DCG-04 blocked cataract formation in cultured $\alpha 3$ (−/−) lenses, suggesting that they have the same permeability properties and inhibit the same critical protease targets as E-64 (data not shown). Affinity labeling of lens homogenates from (+/+) or $\alpha 3$ (−/−) mice using ^{125}I-DCG-03 or ^{125}I-DCG-04 yielded a distinct labeling pattern (Fig. 2*B*, *black arrows*). The labeling of polypeptides by DCG-03 and DCG-04 occurred only in the presence of 1 mM free calcium (Fig. 2*B*). In contrast, a proteasome-specific probe, ^{125}I-NLVS, labeled proteasome subunits regardless of calcium concentration. There was no significant difference in the intensity of E-64-labeled polypeptides in (+/+) and $\alpha 3$ (−/−) lenses, suggesting that the calcium-regulated cysteine proteases targeted by the probes are present at similar levels in both the knock-out and wild type lenses. Furthermore, the activity of all of the predominant labeled proteases (82, 80, 62, and 32 kDa) showed dose-dependent response to addition of free calcium to the extract (Fig. 2*C*). Their activities showed the greatest response within the physiologically relevant range of calcium concentrations (0–0.5 mM). Furthermore, the 62-kDa protease showed a sharp increase in activity within this concentration range, indicating that its activity is likely to be significantly affected even by minor changes in the level of intracellular calcium within the lens.

To further evaluate the role of cysteine protease activation in $\alpha 3$ (−/−) cataract formation, DCG-04 was used for *in situ* affinity labeling of intact lenses. Cultured lenses from 10-day-old mice were incubated for 6 h in the presence of 50 μM DCG-04 followed by homogenization of lenses, SDS-PAGE, and affinity blotting for biotin (Fig. 3*A*). The pattern of labeled polypeptides obtained from $\alpha 3$ (−/−) lenses was identical to that observed in the *in vitro* labeling experiments, indicating that the same protein species are targeted by both labeling methods (compare Fig. 3*A* to Fig. 2*B*). However, in contrast to the labeling *in vitro*, *ex vivo* DCG-04 treatment yielded markedly increased labeling of specific polypeptides in $\alpha 3$ (−/−) lenses (Fig. 3*A*). Measurement of ^{125}I-DCG-04 uptake in lenses of 2-week-old $\alpha 3$ (−/−) and WT mice confirmed that labeling differences did not result from changes in the permeability of the lens (data not shown). Competition with E-64 completely blocked labeling of all polypeptides, indicating that DCG-04-labeled proteins are also the primary targets of E-64. Since covalent modification of targets by affinity labeling reagents requires enzymatic activity, labeling intensity provides a direct indication of the levels of active proteases present in the sample. Therefore, these observations suggest that the activity of a calcium-regulated cysteine protease is significantly increased in the $\alpha 3$ (−/−) lens.

One of the unique properties shared by calpains is their ability to catalyze autoprocessing of mature high molecular weight enzymes to smaller fragments (17). Immunoprecipitation experiments were performed using antisera selective for the three predominant calpains expressed in the lens (m-calpain, μ-calpain, and Lp82) to identify the labeled polypeptides and to determine if some of the proteins were fragments generated by autocatalytic processing (Fig. 3*B*). Immunoprecipitation analyses of DCG-04-labeled $\alpha 3$ (−/−) lenses identified the 82-, 62-, and 32-kDa polypeptides as components derived from Lp82. Similarly, the 80-kDa DCG-04-labeled polypeptide was identified as m-calpain. Following immunoprecipitation of m-calpain, an additional 43-kDa band was observed that is likely to represent a previously described breakdown product of m-calpain (17).

A 62-kDa fragment of Lp82 has been suggested to be the active form of the enzyme (23). To determine if this fragment was being autocatalytically produced in the lens, DCG-04-modified, full-length Lp82 was immunoprecipitated and then incu-

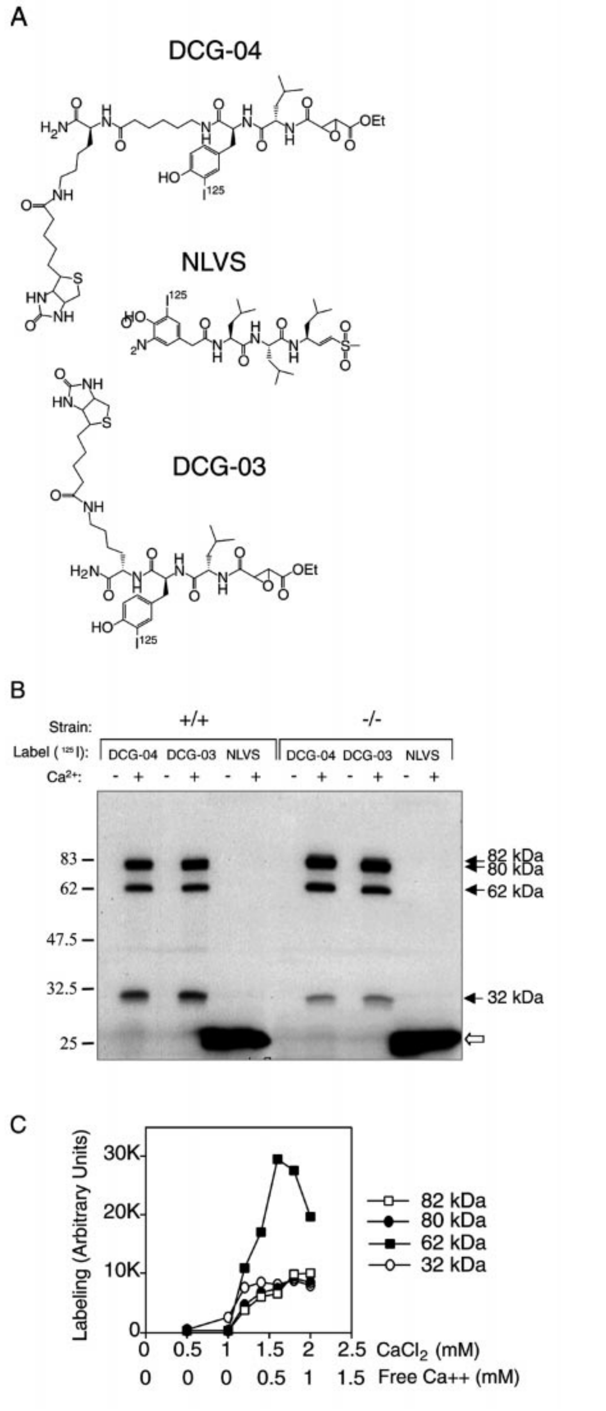

FIG. 2. **Affinity labeling of papain family cysteine proteases in lens homogenates.** *A*, structures of the E-64-derived affinity labeling reagents DCG-03, DCG-04, and the proteasome label NLVS. *B*, affinity labeling of homogenates from WT and α3 (−/−) lenses with ^{125}I-labeled DCG-03, DCG-04, or NLVS in the presence (+) or absence (−) of 1 mM free calcium. Labeled homogenates were separated on a 12.5% acrylamide gel, and labeled polypeptides visualized by autoradiography. *Black arrows* indicate DCG-04- and DCG-03-labeled bands. The *open arrow* indicates the ∼25-kDa catalytic subunits of the proteasome. Molecular weight standards are indicated to the *left*. *C*, quantitation of labeling intensity of each of the major protease species (82, 80, 62, and 32 kDa) in wild-type lens extracts in the presence of increasing concentrations of free calcium. Free calcium concentrations are indicated. Labeling intensity was measured by phosphoimaging of SDS-PAGE gels that had been labeled as in *B*.

bated for 5 min in the presence or absence of 0.5 mM free calcium (Fig. 3*C*). Intact Lp82 was processed to produce the active site-containing 62-kDa fragment only in the presence of

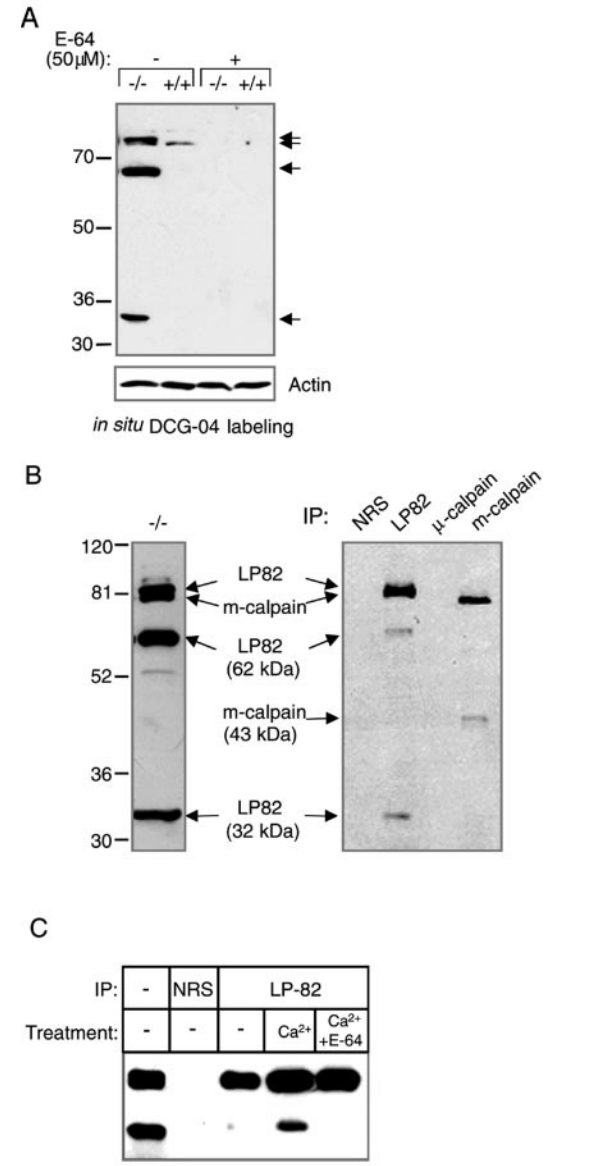

FIG. 3. **Identification of Lp82 and m-calpain as the primary targets of E-64 in the lens.** *A*, intact lenses from 2-week-old α3 (−/−) or WT mice were labeled *in situ* with 50 μM DCG-04 for 6 h. Incubation was performed in the presence or absence of E-64 as indicated. Total lens lysates were separated on a 9% gel, blotted, and probed for biotin by affinity blot. The blot was re-probed with anti-F-actin antibodies to ensure equal loading (*bottom panel*). *B*, homogenates of DCG-04 *in situ*-labeled lenses from 2-week-old α3 (−/−) mice were directly analyzed by affinity blotting for biotin (*left panel*) or subjected to immunoprecipitation using anti-Lp82, anti-μ-calpain, or anti-m-calpain antibodies followed by affinity blotting (*right panel*). Molecular size standards are indicated on the *left side* of the panel (in kDa). *Arrows* indicate the different activated protease bands. *C*, homogenates of DCG-04-labeled lens from 2-week-old α3 (−/−) mice were either directly analyzed by affinity blotting for biotin (*left lane*) or subjected to immunoprecipitation using normal serum or anti-Lp82 antibodies. Immunoprecipitated Lp82 was incubated for 5 min in the presence or absence of 100 μM free calcium. As an additional control, E-64 was added to a final concentration of 50 μM (*right lane*). Immmunoprecipitants were subsequently analyzed by SDS-PAGE, blotted, and probed for biotin.

calcium. Addition of E-64 completely inhibited this processing event.

In order to track expression and activation of m-calpain and Lp82 during initiation of cataractogenesis, α3 (−/−) and WT intact lenses dissected from 1-, 2-, 3-, and 4-week-old mice were affinity-labeled *in situ* with DCG-04 (Fig. 4*A*). Activity profiles

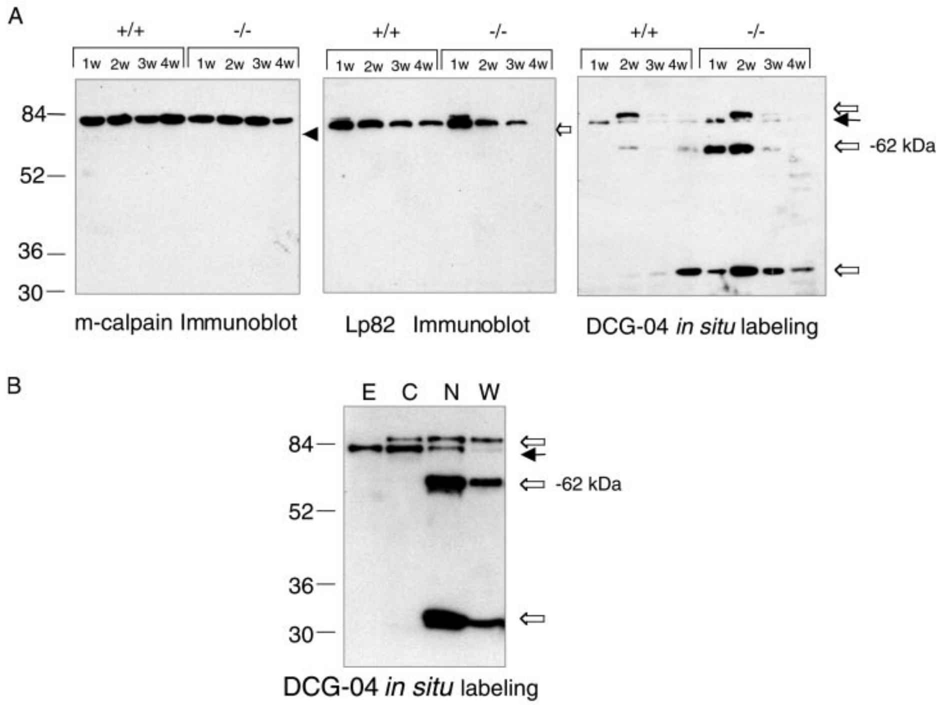

FIG. 4. **Profiling protease activity during cataractogenesis in intact α3 (−/−) lenses.** *A*, intact lenses from 1-, 2-, 3-, and 4-week-old α3 (−/−) or WT mice were incubated with 50 μM DCG-04 for 6 h. Total lysate from labeled lenses was separated by SDS-PAGE, blotted, and probed for biotin. The same blot was reprobed with anti-Lp82 or anti-m-calpain antibodies. *B*, intact lenses from 2-week-old α3 (−/−) or WT mice were incubated with 50 μM DCG-04 for 6 h. The epithelial (*E*), cortical (*C*), and nuclear (*N*) regions of the lens were dissected, separated on a 9% acrylamide gel, and subsequently blotted and probed for biotin. *Upper*, *middle*, and *lower open arrows* correspond to the intact, 62-kDa form, and 32-kDa form of Lp82, respectively. *Black arrow* indicates activated m-calpain.

were compared with protein levels of Lp82 and m-calpain determined in the same samples by immunoblotting. These results indicated that m-calpain activity reached a peak at 1 week of age and was only slightly elevated in the α3 (−/−) lens compared with the WT lens. In contrast, Lp82 activity peaked at 2 weeks of age in both the WT and α3 (−/−) lenses and was significantly elevated in the α3 (−/−) lenses. This increased activity of Lp82 was confirmed by the appearance of the affinity-labeled 62-kDa active form, which could be detected as early as 1 week of age in the α3 (−/−) lenses with no measurable activity observed in the parallel WT lenses. Immediately following peak activation, Lp82 activity decayed gradually and was undetectable by 4 weeks in the α3 (−/−) lenses, consistent with previous reports regarding Lp82 expression in the mouse lens (23). Notably, in the α3 (−/−) lenses intact Lp82 could no longer be detected by 3 weeks of age (Fig. 4*A*, *middle panel*). This expression pattern is consistent with the rapid activation of Lp82 and the accumulation of its degradation products (which are not recognized by the antibody). The m-calpain expression levels, on the other hand, were not altered with age and did not differ significantly between WT and α3 (−/−) lenses (Fig. 4*A*, *right panel*). These results suggest that, although protein levels of both m-calpain and Lp82 are nearly equivalent in WT and α3 (−/−) lenses, Lp82 is activated during α3 (−/−) cataract formation.

To determine the spatial distribution of Lp82 activity within the lens, 2-week-old α3 (−/−) knock-out lenses were labeled with DCG-04 and individual lens regions dissected. Analysis of protease activity indicated that m-calpain activity was located predominantly in the epithelial and cortical regions of the lens, while Lp82 activity was found predominantly in the nuclear region (Fig. 4*B*), further supporting a central role for Lp82 in α3 (−/−) cataractogenesis.

To determine whether the protease activity profiles observed for *ex vivo* cataract formation correlated with cataract formation *in vivo*, cultured lenses were labeled with DCG-04 after various incubation times. Activation of Lp82 occurred within 1 day of lens culture and reached a peak at 2 days. This activation profile coincided with the time frame for cataract initiation *in vivo*. Furthermore, the activity profile of Lp82 in cultured lenses was similar to the labeling profile observed for lenses in which cataract formation took place *in vivo* (data not shown).

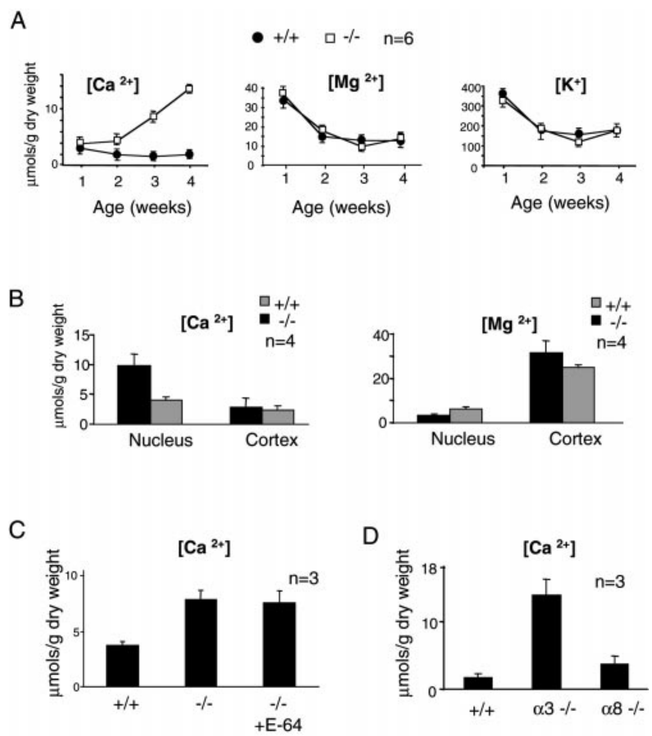

FIG. 5. **Ca^{2+} accumulates in the nuclear region of lenses from α3 (−/−) mice.** *A*, lenses from WT and α3 (−/−) mice at the indicated ages were vacuum-dried, weighed, and solubilized in 2% nitric acid for 12 h. The content of calcium, magnesium, and potassium was determined using atomic emission spectroscopy. All measurements were normalized to lens dry weight. *B*, calcium and magnesium levels of the nuclear and the cortical regions of lenses from 10-day-old WT and α3 (−/−) mice. *C*, determination of calcium levels in cultured WT, α3 (−/−), or E-64-treated lenses following 1 week of incubation. *n* represents the number of mice analyzed in each experiment. *D*, calcium measurements of lenses from 1-month old WT, α3 (−/−), and α8 (−/−) mice.

Effect of Gap Junction Disruption on Calcium Flux in the

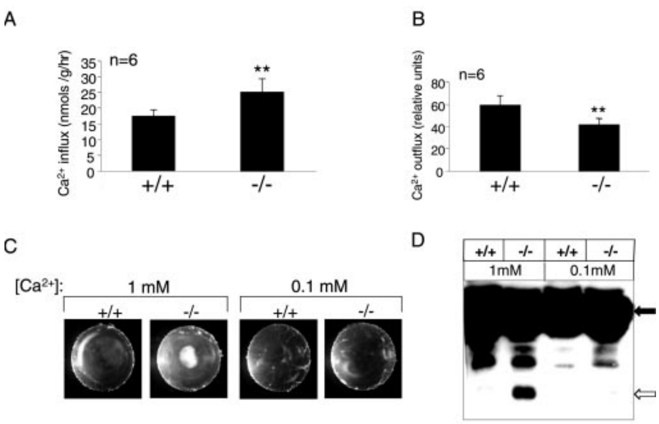

FIG. 6. **Lack of $\alpha 3$ gap junctions results in increased influx and reduced outflux of calcium ions into the lens.** *A*, 12 lenses from WT and $\alpha 3$ (−/−) mice were incubated in the presence of AAH containing 2 μCi of ^{45}Ca. After 2 h of incubation at 37 °C, each lens was washed extensively in AAH and solubilized for 1 h using tissue solubilizer solution. Radioactivity in solubilized lenses was determined using a β-counter. *B*, 12 pairs of lenses from WT and $\alpha 3$ (−/−) mice were incubated in the presence of ^{45}Ca. After 2 h of incubation, lenses were washed extensively and placed in a fresh non-radioactive AAH. Lens and medium radioactivity was determined after 2 h of incubation. Relative units were calculated by subtracting the final lens counts per minute (cpm) from the initial lens cpm and dividing this number by the initial lens cpm. Averages were calculated using the data obtained from each individual pair. *Asterisks* (**) denote a significant difference (P values < 0.01) from WT as determined by a non-parametric unpaired Mann-Whitney statistical test. *C*, lenses from 1-week-old $\alpha 3$ (−/−) or WT mice incubated for 2 days in 199 medium containing 1 or 0.1 mM free calcium. *D*, Western blot analyses of total lens homogenates (corresponding to the lenses in *panel C*) using anti-γ-crystallin antibodies. *Closed arrows* indicate the intact γ-crystallin, and *open arrows* indicate the cleaved form of γ-crystallin.

Lens—The finding that calcium-dependent cysteine proteases were hyperactivated in $\alpha 3$ connexin-deficient lenses suggested that $\alpha 3$ gap junctions play an important role in maintaining calcium homeostasis of the lens. To investigate this possibility, levels of Ca^{2+}, Mg^{2+}, and K^+ ions in WT and $\alpha 3$ (−/−) lenses were measured using optical emission spectroscopy (Fig. 5). Lenses from $\alpha 3$ (−/−) mice exhibited a dramatic age-dependent increase in the levels of Ca^{2+} with no marked change in the levels of Mg^{2+} and K^+ (Fig. 5*A*). This increase in Ca^{2+} in the $\alpha 3$ (−/−) lenses was mainly due to accumulation of Ca^{2+} in the nuclear region of the lens (Fig. 5*B*). Cultured lenses from 1-week-old $\alpha 3$ (−/−) mice also exhibited increased calcium accumulation compared with cultured WT lenses (Fig. 5*C*). Significantly, *ex vivo* treatment with E-64 did not affect lens calcium levels, suggesting that protease activation acts downstream of calcium accumulation during cataractogenesis.

In contrast to the $\alpha 3$ (−/−) lenses, which generate severe cataracts, deletion of $\alpha 8$ connexin results in microphthalmia accompanied by a mild cataract. Ca^{2+} levels measured in lenses from 1-month-old $\alpha 8$ (−/−) mice were only slightly elevated relative to WT levels and were substantially lower that the levels observed for age-matched $\alpha 3$ (−/−) lenses (Fig. 5*D*). This result suggests that $\alpha 3$ and $\alpha 8$ gap junctions may have distinct functions in the lens and that cataract severity is correlated with calcium accumulation.

To gain further insight into the role of $\alpha 3$ gap junctions in maintaining calcium homeostasis, Ca^{2+} influx and outflux rates were measured. In this assay, pre-cataractous, clear lenses from 8-day-old mice were examined. The influx and outflux rates were measured using ^{45}Ca as a tracer. For Ca^{2+} influx measurements, lenses were incubated in an artificial aqueous humor containing ^{45}Ca. Following 2 h of incubation, $\alpha 3$ (−/−) lenses exhibited a 30% increase in the calcium influx rate compared with WT (Fig. 6*A*, *left panel*). To determine calcium outflux, lenses pre-loaded with ^{45}Ca were placed in a non-radioactive artificial aqueous humor. After 2 h of incubation, radioactivity was measured in both the medium and the lens. A 30% decrease in outflux rate was observed in $\alpha 3$ (−/−) lenses compared with WT lenses (Fig. 6*A*, *right panel*). In both influx and outflux assays, statistical significance was determined by non-parametric unpaired Mann-Whitney test. Thus, the observed accumulation of calcium in the nuclear region of the $\alpha 3$ (−/−) lens resulted from perturbations in calcium flux.

To further clarify the role of calcium flux in protein degradation and lens cataractogenesis, $\alpha 3$ (−/−) lenses were cultured in the presence of reduced calcium concentrations relative to normal levels in culture media. At low extracellular Ca^{2+} concentrations, a smaller gradient between the extracellular and intracellular compartments exists, leading to a lower Ca^{2+} influx rate. Lenses from 1-week-old $\alpha 3$ (−/−) mice cultured in the presence of 1 mM final Ca^{2+} developed cataracts within 2 days, whereas lenses that were exposed to a 10-fold reduced concentration of free Ca^{2+} remained transparent (Fig. 6*C*). Of the 20 lenses cultured in the presence of 0.1 mM Ca^{2+}, only 2 developed a mild cataract within 2 days, whereas all 20 lenses incubated under 1 mM Ca^{2+} showed sever nuclear opacity. γ-Crystallin cleavage, monitored after 2 days of incubation, correlated with the formation of nuclear cataracts (Fig. 6*D*).

DISCUSSION

Several targeted gene disruption studies have examined the significance of intercellular communication mediated by gap junctions (2, 23, 24). However, the mechanisms that link connexin function to related phenotypic changes are not clear. Connexin knockout mice provide an advantageous model for the exploration of the physiological role of cell-cell communication in the lens. In this report, we demonstrate a role for $\alpha 3$ connexin in maintenance of calcium homeostasis in the lens. Deletion of $\alpha 3$ gap junctions leads to accumulation of calcium in the nuclear region of the lens and the subsequent activation of calcium-dependent cysteine proteases. In particular, activation of the lens-specific calpain Lp82 initiates nuclear cataract formation, presumably through increasing cleavage of lens γ-crystallin, resulting in its aggregation (Fig. 7).

Calcium-dependent Cysteine Proteases Are Activated during $\alpha 3$ (−/−) Cataractogenesis—In this study we show that protease activation is a key event during cataract formation in $\alpha 3$ connexin-deficient mice. This conclusion is supported by three observations. (*a*) γ-Crystallin cleavage products accumulate in lenses from $\alpha 3$ (−/−) mice. (*b*) The general cysteine protease inhibitor, E-64, blocks both cataract formation and crystalline cleavage in cultured $\alpha 3$ (−/−) lenses. (*c*) Lp82 is a primary target of E-64 in the lens, and its activity is abnormally elevated during cataractogenesis in $\alpha 3$ (−/−) lenses.

In vitro affinity labeling in the presence and absence of free calcium demonstrated that the E-64 analog DCG-04 exclusively labeled proteases that required calcium for enzymatic activity. Our inability to detect labeled polypeptides in extracts prepared in the absence of calcium suggests that calpains are the predominant papain family cysteine proteases in the lens. The *in vitro* DCG-04 labeling also indicates that there is no significant difference in the expression levels of calpains in $\alpha 3$ (−/−) compared with WT lenses, as in both cases calpains are expressed and can be readily activated by the presence of calcium.

Activation of calpains during the process of cataractogenesis has been extensively studied both in humans and in various mouse models (25–27). Three different calpains have been shown to be expressed in the lens, including m-calpain and the recently discovered lens-specific calpains, Lp82 and Lp85 (17,

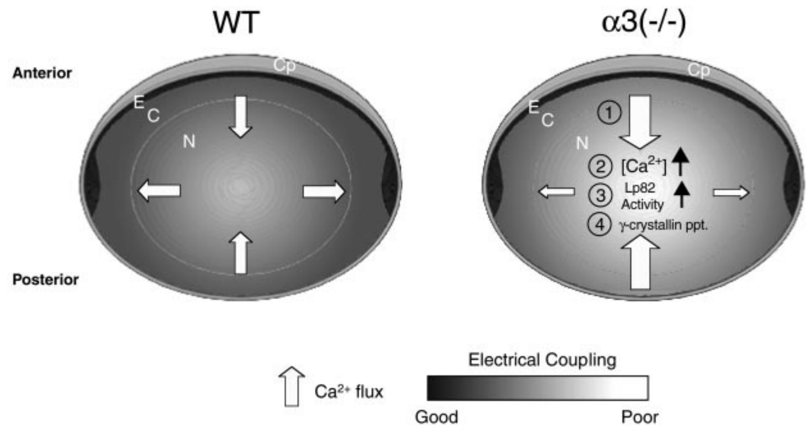

FIG. 7. **The molecular events leading to cataract formation in the α3 (−/−) lens.** *1*, loss of α3 gap junctions leads to perturbations in lens calcium flux; *2*, calcium accumulates in the lens nuclear region; *3*, calcium activates the lens-specific calpain, Lp82, in the nuclear region; *4*, γ-crystallin is cleaved forming insoluble aggregates causing lens opacity and reduced electrical coupling. *Cp*, *E*, *C*, and *N* designate the capsule, epithelial layer, lens cortical region, and nuclear region, respectively.

23, 28). μ-Calpain, on the other hand, is poorly expressed in the lens. Both m-calpain and Lp82 were active during α3 (−/−) cataractogenesis. However, the most apparent difference in protease activity profiles between α3 (−/−) and WT lenses was the presence of a 62-kDa form of Lp82 that is generated by proteolytic processing of the full-length protein. It has been postulated that this 62-kDa form of Lp82 represents the predominant active form of the enzyme (23). The fact that we detected the 62-kDa form of Lp82 as early as 1 week of age in α3 (−/−) mice prior to detection of active, full-length Lp82 suggests that the processed form requires lower levels of calcium for its activation. These observations, together with the finding that the activity of the 62-kDa form correlates spatially and temporally with cataract initiation, suggest that Lp82 is the principal protease responsible for cataractogenesis in the α3 (−/−) lens.

During α3 (−/−) cataract progression, there is an accumulation of γ-crystallin cleavage products likely to be important for cataract formation. The same cleavage of γ-crystallin between residues Asp^{73} and Ser^{74} during α3 (−/−) cataractogenesis is also observed in cases of human cataracts (13). Furthermore, Asp^{73} to Gly mutations found in CAT2 mice result in a nuclear cataract (29), and expression of truncated forms of γ-crystallin is associated with human hereditary Coppock-like cataracts (30). These results suggest that this region within γ-crystallin is important for maintaining the correct folding and hence the solubility of the protein.

Although we were able to demonstrate that peak enzymatic activity of Lp82 coincides with the appearance of γ-crystallin cleavage products, we cannot rule out the possibility that other proteases are directly responsible for this cleavage event. However, the fact that E-64 and DCG-04 both inhibit γ-crystallin cleavage indicates that calpain activation takes place upstream of γ-crystallin processing. Calpain activation in the lens may serve as a means to activate additional downstream proteases that are the direct effectors of γ-crystallin cleavage.

α3 Gap Junctions Play a Role in Maintaining Calcium Homeostasis in the Lens—In order to maintain a clear lens, the ionic environment must support the folding and stabilization of crystallins. Since the lens as an avascular organ, it requires cellular mechanisms to ensure metabolite transport to all cells. Deletion of α3 gap junctions results in an increase in total calcium in the nuclear region of the lens. This increase in nuclear calcium is due to both reduced calcium outflux from the lens and increased calcium influx into the lens. Reduced outflux of calcium in the (−/−) lens suggests a role for α3 gap junctions in mediating the outward flow of ions. It is clear that members of the gap junction family mediate the transport of calcium ions (31). In addition, it has been suggested that α3 hemi-channels mediate transfer of cations rather than anions (32).

The notion that gap junctions can mediate the transfer of ions was previously suggested in a model for ion current flow in the lens (33). According to this model, the inward ion flow is driven by the concentration gradient between the intra- and extracellular spaces, whereas outflux of ions from the lens is facilitated by gap junctions. Consistent with this model, our findings show that calcium accumulation in α3 (−/−) lenses is partially due to a decrease in the outflux rate in mutant lenses. This finding is also in line with conductivity measurements that show loss of electrical coupling between the nuclear fiber cells of the α3 (−/−) lens (34). This uncoupled zone in the α3 (−/−) lens corresponds to the zone of cataract formation. Furthermore, the lack of coupling in the nuclear region of α3 (−/−) lens suggests that other lens fiber connexins, such as α8, cannot rescue electrical coupling in this region. As suggested previously, the absence of functional α8 gap junctions in the nuclear region of the α3 (−/−) lens could be due to connexin degradation or gap junction gating triggered by the presence of high calcium levels (35, 36).

Other mechanisms for maintenance of calcium levels in the lens might also exist. For example, altered regulation of both selective and non-selective ion channels such as L-type calcium channels and Na^+-Ca^{2+} exchangers may have a critical role in calcium homeostasis (37). It is unlikely, however, that ATPase pumps are involved in ion mobilization within the lens nuclear region, mainly due to the low metabolic activity in this region (38).

Our data also indicate that the rate of calcium influx is higher in the α3 (−/−) lens. In many model systems, cataract formation is followed by increased lens permeability, which subsequently leads to calcium accumulation. However, since influx measurements were performed on transparent, pre-cataractous lenses from 8-day-old α3 (−/−) mice, increased permeability is not likely to be the explanation for increased calcium levels in our model. A possible explanation for this observation may lie in the role of gap junctions as integral membrane proteins that are important for the overall cellular architecture of the lens. Thus, it is plausible that alterations in the membrane structure resulting from reduction in the levels of gap junctions affects lens permeability and hence the flux of ions along the concentration gradient. It is also likely that the lack of gap junctions in the lens affects the distribution of other cytoskeletal proteins or membrane components. These issues will be the focus of future studies.

In summary, the data presented here propose a role for α3 gap junctions in maintaining calcium homeostasis in the lens. The recently reported α3-linked congenital cataract suggests a similar role for gap junctions in humans. Moreover, both calcium accumulation and γ-crystallin cleavage were found to be predominant features of human senile cataracts. Therefore, it will be important to assess the expression and function of lens connexins and calpains in human senile cataracts.

Acknowledgments—We thank Thomas Shearer, John Elce, Sivia Bar-Noy, and Nechama Kosower for kind gifts of reagents. We thank Zena Werb, Peter Walter, and Ira Herskawitz for critical evaluation of the manuscript.

REFERENCES

1. Kumar, N. M., and Gilula, N. B. (1996) *Cell* **84,** 381–388
2. Lo, C. W. (1999) *Dev. Genet.* **24,** 1–4
3. White, T. W., and Bruzzone, R. (2000) *Brain. Res. Brain. Res. Rev.* **32,** 130–137
4. Goodenough, D. A. (1992) *Semin. Cell Biol.* **3,** 49–58
5. Church, R. L., Wang, J. H., and Steele, E. (1995) *Curr. Eye Res.* **14,** 979–981
6. Paul, D. L., Ebihara, L., Takemoto, L. J., Swenson, K. I., and Goodenough, D. A. (1991) *J. Cell Biol.* **115,** 1077–1089
7. Gong, X., Li, E., Klier, G., Huang, Q., Wu, Y., Lei, H., Kumar, N. M., Horwitz, J., and Gilula, N. B. (1997) *Cell* **91,** 833–843
8. White, T. W., Goodenough, D. A., and Paul, D. L. (1998) *J. Cell Biol.* **143,** 815–825
9. Pal, J. D., Liu, X., Mackay, D., Shiels, A., Berthoud, V. M., Beyer, E. C., and Ebihara, L. (2000) *Am. J. Physiol.* **279,** C596–C602
10. Shiels, A., Mackay, D., Ionides, A., Berry, V., Moore, A., and Bhattacharya, S. (1998) *Am. J. Hum. Genet.* **62,** 526–532
11. Horwitz, J., Bova, M. P., Ding, L. L., Haley, D. A., and Stewart, P. L. (1999) *Eye* **13,** 403–408
12. Mandal, K., Chakrabarti, B., Thomson, J., and Siezen, R. J. (1987) *J. Biol. Chem.* **262,** 8096–8102
13. Srivastava, O. P., and Srivastava, K. (1998) *Biochem. Biophys. Res. Commun.* **253,** 288–294
14. Stephan, D. A., Gillanders, E., Vanderveen, D., Freas-Lutz, D., Wistow, G., Baxevanis, A. D., Robbins, C. M., VanAuken, A., Quesenberry, M. I., Bailey-Wilson, J., Juo, S. H., Trent, J. M., Smith, L., and Brownstein, M. J. (1999) *Proc. Natl. Acad. Sci. U. S. A.* **96,** 1008–1012
15. Truscott, R. J., Marcantonio, J. M., Tomlinson, J., and Duncan, G. (1990) *Invest. Ophthalmol. Vis. Sci.* **31,** 2405–2411
16. Paterson, C. A., Zeng, J., Husseini, Z., Borchman, D., Delamere, N. A., Garland, D., and Jimenez-Asensio, J. (1997) *Curr. Eye Res.* **16,** 333–338
17. Azuma, M., Fukiage, C., David, L. L., and Shearer, T. R. (1997) *Exp. Eye Res.* **64,** 529–538
18. Shearer, T. R., Ma, H., Fukiage, C., and Azuma, M. (1997) *Mol. Vis.* **3,** 8
19. Azuma, M., David, L. L., and Shearer, T. R. (1992) *Biochim. Biophys. Acta* **1180,** 215–220
20. Greenbaum, D., Medzihradszky, K. F., Burlingame, A., and Bogyo, M. (2000) *Chem Biol* **7,** 569–581
21. Bogyo, M., McMaster, J. S., Gaczynska, M., Tortorella, D., Goldberg, A. L., and Ploegh, H. (1997) *Proc. Natl. Acad. Sci. U. S. A.* **94,** 6629–6634
22. Thomas, G. R., Sanderson, J., and Duncan, G. (1999) *J. Physiol.* **516,** 191–199
23. Ma, H., Hata, I., Shih, M., Fukiage, C., Nakamura, Y., Azuma, M., and Shearer, T. R. (1999) *Exp. Eye. Res.* **68,** 447–456
24. Plum, A., Hallas, G., Magin, T., Dombrowski, F., Hagendorff, A., Schumacher, B., Wolpert, C., Kim, J., Lamers, W. H., Evert, M., Meda, P., Traub, O., and Willecke, K. (2000) *Curr. Biol.* **10,** 1083–1091
25. Andersson, M., Sjostrand, J., and Karlsson, J. O. (1996) *Ophthalmic Res.* **28,** 51–54
26. Nixon, R. A., Saito, K. I., Grynspan, F., Griffin, W. R., Katayama, S., Honda, T., Mohan, P. S., Shea, T. B., and Beermann, M. (1994) *Ann. N. Y. Acad. Sci.* **747,** 77–91
27. Sanderson, J., Marcantonio, J. M., and Duncan, G. (1996) *Biochem. Biophys. Res. Commun.* **218,** 893–901
28. Ma, H., Shih, M., Hata, I., Fukiage, C., Azuma, M., and Shearer, T. R. (2000) *Curr. Eye Res.* **20,** 183–189
29. Klopp, N., Favor, J., Loster, J., Lutz, R. B., Neuhauser-Klaus, A., Prescott, A., Pretsch, W., Quinlan, R. A., Sandilands, A., Vrensen, G. F., and Graw, J. (1998) *Genomics* **52,** 152–158
30. Brakenhoff, R. H., Henskens, H. A., van Rossum, M. W., Lubsen, N. H., and Schoenmakers, J. G. (1994) *Hum Mol Genet* **3,** 279–283
31. Paemeleire, K., Martin, P. E., Coleman, S. L., Fogarty, K. E., Carrington, W. A., Leybaert, L., Tuft, R. A., Evans, W. H., and Sanderson, M. J. (2000) *Mol. Biol. Cell* **11,** 1815–1827
32. Trexler, E. B., Bennett, M. V., Bargiello, T. A., and Verselis, V. K. (1996) *Proc. Natl. Acad. Sci. U. S. A.* **93,** 5836–5841
33. Robinson, K. R., and Patterson, J. W. (1982) *Curr. Eye Res.* **2,** 843–847
34. Gong, X., Baldo, G. J., Kumar, N. M., Gilula, N. B., and Mathias, R. T. (1998) *Proc. Natl. Acad. Sci. U. S. A.* **95,** 15303–15308
35. Lin, J. S., Fitzgerald, S., Dong, Y., Knight, C., Donaldson, P., and Kistler, J. (1997) *Eur. J. Cell Biol.* **73,** 141–149
36. Crow, J. M., Atkinson, M. M., and Johnson, R. G. (1994) *Invest. Ophthalmol. Vis. Sci.* **35,** 3332–3341
37. Srivastava, S. K., Wang, L. F., Ansari, N. H., and Bhatnagar, A. (1997) *Invest. Ophthalmol. Vis. Sci.* **38,** 2300–2312
38. Mathias, R. T., Rae, J. L., and Baldo, G. J. (1997) *Physiol. Rev.* **77,** 21–50